Desalination and Water Treatment
www.deswater.com
doi: 10.1080/19443994.2014.971617

53 (2015) 2324–2338
March

Taylor & Francis
Taylor & Francis Group

Assessment of seawater intrusion potential from sea-level rise and groundwater extraction in a coastal aquifer

Hai Van Pham[a], Sang-Il Lee[b,*]

[a]*Department of Civil and Environmental Engineering, Louisiana State University, Baton Rouge, LA 70803, USA*
[b]*Department of Civil and Environmental Engineering, Dongguk University, 3-26, Pil-dong, Jung-gu, Seoul 100-715, South Korea, Tel. +82 222603353; Fax: +82 222668753; email: islee@dongguk.edu (S.-I. Lee)*

Received 5 November 2013; Accepted 14 December 2013

ABSTRACT

Groundwater is an important water resource in many coastal areas around the world. Excessive pumping can change the flow pattern so that seawater may migrate into the freshwater aquifer. In addition, the rise of the sea level due to climate change could accelerate the landward intrusion of seawater. This study addresses the problem of variable-density groundwater flow and miscible salt transport to assess the potential of seawater intrusion in coastal aquifers. Our conceptual model considers a complete hydrogeologic system including the river system, the seasonal groundwater recharge, the groundwater pumping, and the interaction between seawater and groundwater. Model calibration is performed using the covariance matrix adaptation–evolution strategy as a robust derivative-free global optimization algorithm. The advantage of this algorithm is its ability to reach a near global solution in solving the groundwater inverse problem, which is typically nonlinear and ill-posed. Simulations for the Nam Dinh Province, Vietnam over the period of 90 years indicate that seawater intrusion will occur, but the extent of it will vary depending on scenarios. The extraction of groundwater is the key factor governing the intrusion of seawater. The magnitude of seawater intrusion caused by rising sea level sturned out to be relatively small. Sensitivity analysis reveals that uncertainties of transport parameters could significantly affect the assessment of seawater intrusion potential.

Keywords: Sea-level rise; Seawater intrusion; Coastal aquifers; Nam Dinh Province; SEAWAT

1. Introduction

Coastal aquifers constitute important sources of freshwater in many parts of the world. Nevertheless, their overexploitation combined with climate change and sea-level rise could disturb the naturally established equilibrium between seawater and freshwater, resulting in uncontrolled saltwater encroachment into coastal aquifers [1].

Seawater intrusion into coastal aquifers is a long-studied problem. However, studies investigating both effects of sea-level rise and groundwater extraction on seawater intrusions have started only recently [2–6]. According to the literature, the magnitude of the impact depends on the site specification such as topography or pumping activities, the method of analysis, and the assumptions made (e.g., consideration of shoreline changes). For the same Nile Delta aquifer, for instance, results from a two-dimensional numerical

*Corresponding author.

modeling show that a 50 cm rise in the Mediterranean sea level will cause additional intrusion of 9 km [2], while the generalized analytical approach reveals an inland migration of 5 km [7].

Many studies find that the effect of groundwater extraction is significant, and much larger than the effect of rising sea levels [2,5,6]. Other studies, however, show that groundwater extraction is not a major cause [4,8]. Overall, it is quite clear that the impacts of rising sea level and groundwater extraction need investigation under site-specific conditions.

Vietnam ranks among the top five most vulnerable countries to climate change and rising sea levels, having more than 3,200 km of coastlines and extensive low-lying coastal areas [9,10]. Here, sea level has risen at the rate of 3 mm/y during 1993–2008 [11]. Prediction for the high development scenario shows a rise of approximately 100 cm by 2100. Saltwater has already penetrated 30–50 km up the Red River and 60–70 km up the Mekong River [12], which are two largest rivers in the north and south of Vietnam.

Recent rapid urbanization, industrialization, and intensification of agriculture have increased water demand [13], causing high pressure for the groundwater exploitation. Significant decrease in groundwater level is reported at intensive pumping areas: in two coastal provinces in northern Vietnam, Thai Binh, and Nam Dinh, the groundwater level has decreased about 4 and 8 m in the period of 1995–2011, respectively. The decline of groundwater levels naturally results in seawater intrusion.

Located in the extreme-east of the Red River Delta, Nam Dinh Province is one of the typical coastal provinces facing the problem of seawater intrusion. Doan et al. [14] used groundwater models to predict the exploitable groundwater reserves and to simulate the movement of the interface between freshwater and brackish water in the Pleistocene aquifers. Their work did not consider the potential of seawater intrusion from the sea and upper aquifers. An up-to-date MODFLOW model was developed to predict the decline of groundwater levels for several scenarios of groundwater pumping [15]. Yet, the model neglected the influence of river systems and groundwater recharge. To the best of our knowledge, none of the previous works has explained the following important issues in this region: (1) How active is the interaction between the surface water and the groundwater? (2) What is the complete mass balance? (3) How much do the sea-level rise and groundwater extraction affect the groundwater level and the transient movement of freshwater/saltwater interface?

In order to assess the potential impacts of sea-level rise and groundwater extraction on the decline of groundwater levels and the intrusion of seawater in a coastal aquifer in Vietnam over the next several decades, we develop a numerical model of variable-density groundwater flow and miscible salt transport based on the USGS computer program SEAWAT. Our conceptual model encompasses a complete hydrogeologic system including the river system, the seasonal groundwater recharge, groundwater pumping, and the interaction between the seawater and the groundwater. We first calibrate the model against eleven-year data-set of historical groundwater levels, and validate the model against another four-year data-set. Then, we run the developed model for different scenarios using the optimized hydraulic parameters. Finally, we conduct the analysis to understand the sensitivity of transport parameters.

2. Description of study area

The study area is the coastal aquifers of the Nam Dinh Province located in the eastern part of the Red River Delta (Fig. 1). The area is 1,130.9 km^2 bounded by the Red River, Dao River, Day River, and has 72 km of coastline. The population in the end of 2010 is 1.83 million. The terrain is relatively flat and gradually inclines to the sea with elevation variations 0.2–3.0 m above the sea level. Areas with an elevation of less than 2 m are often flooded by heavy rain. The land use is dominated by rice fields (58%), urban and rural areas (16%), water bodies (11%), and fish and shrimp aquacultures using fresh and brackish water (5%) [16], having high groundwater recharge potential.

The study area has a tropical monsoon climate characterized by a wet season (May to September) and a dry season (October to April). Most precipitation prevails in the wet season (more than 88%) and the rate of evaporation is about 70%. The average annual rainfall and evaporation are 1,690 mm and 817 mm, respectively. As an example, Fig. 2(A) shows the monthly average rainfall and evaporation variations at Ninh Binh station.

There is a highly dense stream network consisting of four large rivers: the Red River, the Dao River, the Ninh Co River, and the Day River (Fig. 1). These rivers are 400–600 m wide and 2–15 m deep. The river water levels vary seasonally and spatially, and the water levels recorded at observation stations far from the sea (Fig. 2(B)) are much higher than the values at stations near the sea (Fig. 2(C)), which explains the general flow direction from the northwest to the southeast.

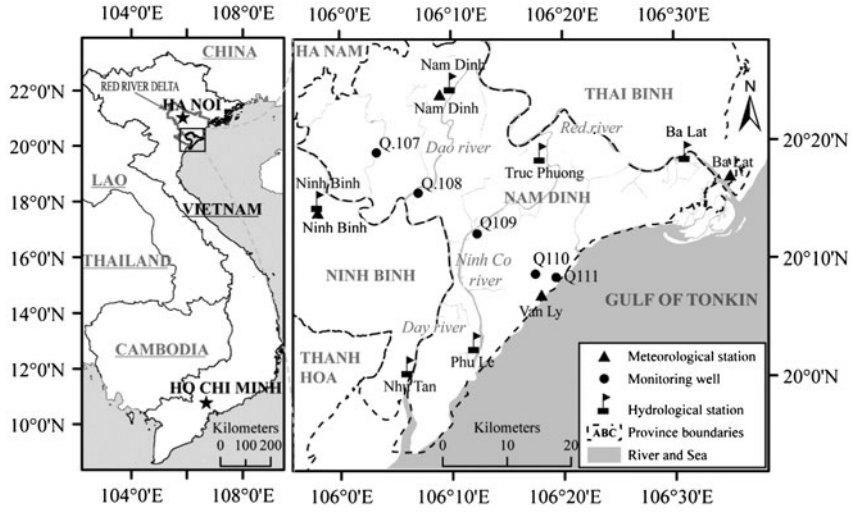

Fig. 1. Map of the study area and monitoring network in Nam Dinh Province and its vicinity.
Source: 2003 Vietnam Water Resources Atlas, National Water Resources Council, Ministry of Natural Resources and Environment.

2.1. Hydrostratigraphy and aquifer properties

There are five available hydrogeological units in the study area (Fig. 3), but only two of them play an economical role as groundwater sources: the Holocene aquifers and the Pleistocene aquifer. The key characteristics of these aquifers are briefly summarized below, based on previous studies [14,15].

The Holocene aquifers distributed widely in the province comprise the upper and the lower aquifer. The upper aquifer is an unconfined aquifer, which consists of sand, silty clay, and clay. The thickness ranges from 2 to 28 m. The main water supply for this aquifer is rainfall and surface water. The lower aquifer is a confined aquifer, interbedded between aquitards. Underlying the Holocene aquifers is the marine aquitard sediments of the Vinh Phuc formation. It is Pleistocene in age and largely distributed in the area. The lithology mainly consists of clay, and silty clay mixed with lateritic gravel. The thickness changes from 20 to 25 m. The Pleistocene confined aquifer is below the marine aquitard sediments and covers the Neogen sediments. This aquifer expands all over the area, not exposed on the surface. It consists mainly of quartz sand, gravel, and pebbles. The depth gradually changes from 80 to 90 m in the central part of the province to 60–70 m in coastal areas. The thickness of the aquifer increases from the inland to the sea, reaching 30–40 m in the coastal areas.

A large fresh water area was discovered in confined aquifers with good water quality in the whole area of Hai Hau, Nghia Hung Districts, the Southern part of Y Yen, Nam Truc, Truc Ninh, and some parts of Xuan Truong, Giao Thuy Districts [14]. There is no convincing evidence of hydraulic connection between the surface and the subsurface waters.

2.2. Likely causes of seawater intrusion

A significant increase in TDS in Holocene aquifers was observed during the period of 1995–2010. TDS at observation well Q111 (several hundred meters from seashore) increased from 6 to 20 g/L, while at observation well Q110 (3.4 km from seashore), TDS increased from 1 to 6 g/L (Fig. 2(E)). In Pleistocene aquifers, the TDS level is relatively low and shows a slight increase. The source of salinity varies. In the unconfined aquifer, the salinity comes from both rivers and the sea, or from leaching of paleo waters in very young marine sediment. In the northern part of the confined aquifers, the salinity is from the unconfined aquifer, through the density-driven transport from relatively high-permeability layers and the diffusive transport from relatively low-permeability layers [18].

Fig. 2(D) illustrates the groundwater levels in Holocene aquifers from 1995 to 2010. At inland observation wells Q107, Q108, and Q109, groundwater levels are relatively stable, showing the seasonality. At observation well Q111 close to the sea, the groundwater levels show an increasing trend and the weak seasonality. In contrast, groundwater levels in the Pleistocene confined aquifer are deceasing dramatically, with slight change between seasons, and have a strong correlation with groundwater extraction (Fig. 4(B)).

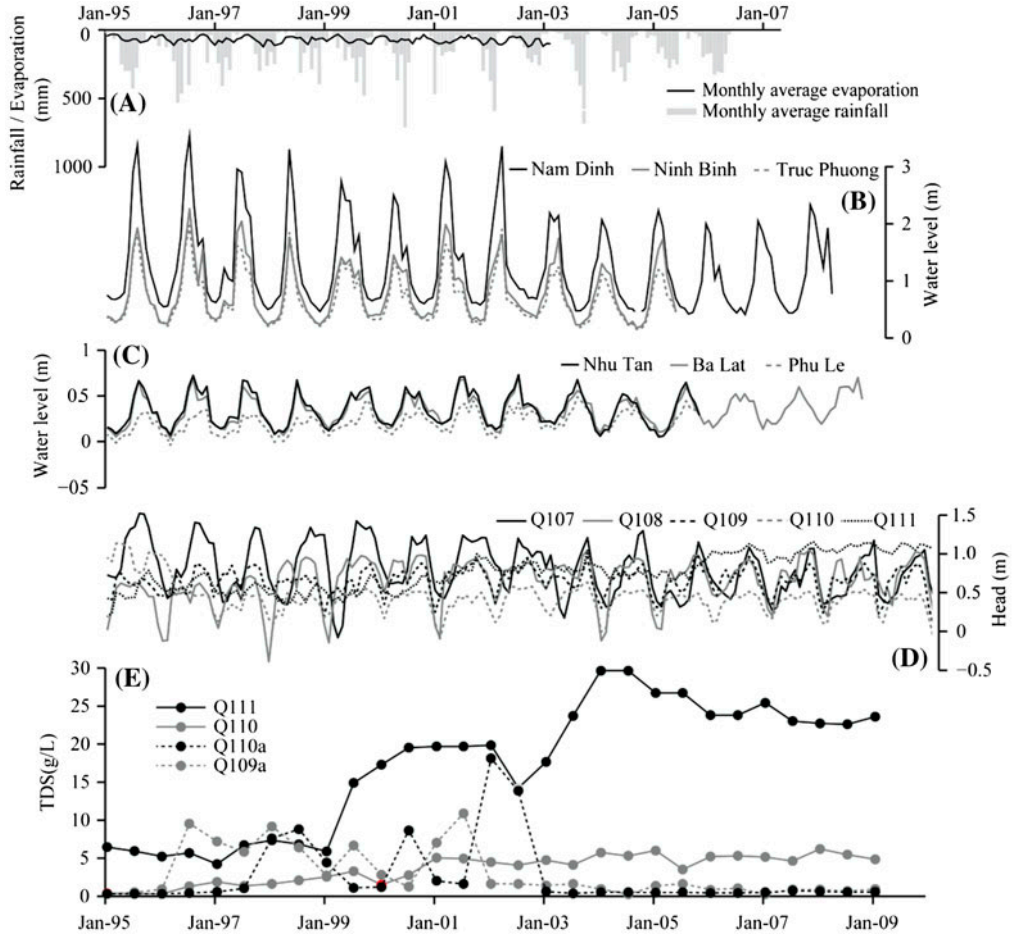

Fig. 2. Hydrometeorology and water quality records for selected monitoring stations: (A) Monthly average rainfall and evaporation for Ninh Binh station; (B) Monthly average river water levels at stations far from the sea; (C) Monthly average river water levels at stations close to the sea; (D) Groundwater levels in Holocene aquifers; and (E) Total dissolved solids (TDS) at stations near the sea. Hydro-meteorological data are from the National Hydro-meteorological Service, MONRE. Groundwater data are from CWRPI, MONRE.

For example, at observation well Q109a, groundwater levels have decreased as much as 9 m from 1995 to 2010, giving a lowering rate of 0.56 m/y. The decline is likely to result in the change of flow patterns in a way that seawater may migrate into the fresh water area.

2.3. Estimation of groundwater exploitation

There are currently two forms of groundwater extraction in Holocene aquifers. Large-scale extraction is popular in Hai Hau, Nghia Hung, and Y Yen district. There, the pumped groundwater is treated before being supplied to households. Small-scale extraction is common in rural areas. The groundwater is exploited from dug wells, which usually have a diameter of 0.8–1.3 m and a depth of 5–10 m. Recently, this type of well is not popular because of poor water quality and seawater intrusion. Since the extracted water is consumed in the neighborhood area and recharged back to the aquifer, we do not take this type of well into account for the model.

Since 1983, with the support from The United Nations Children's Fund (UNICEF), the clean water program for rural areas has established thousands of "UNICEF-drills". These wells have a diameter of 50–150 mm and are usually drilled down into confined aquifers at a depth of 50–130 m. Households extract groundwater based on their demand and do not have any specific plan for sustainable use. In some districts, such as Hai Hau, Nghia Hung, 100% of residents are using water from these wells. This type of well has increased dramatically since 1998 because of its low cost and improvement in technology (Table 1). This

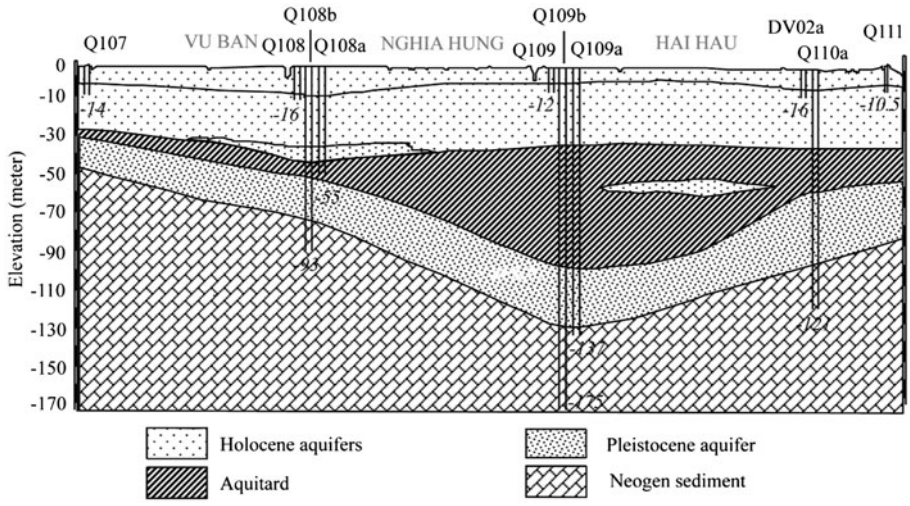

Fig. 3. Typical cross-section of the study area: Northwest–Southeast cross-section passing the national groundwater monitoring wells from Vu Ban district to Hai Hau district. Modified after [17].

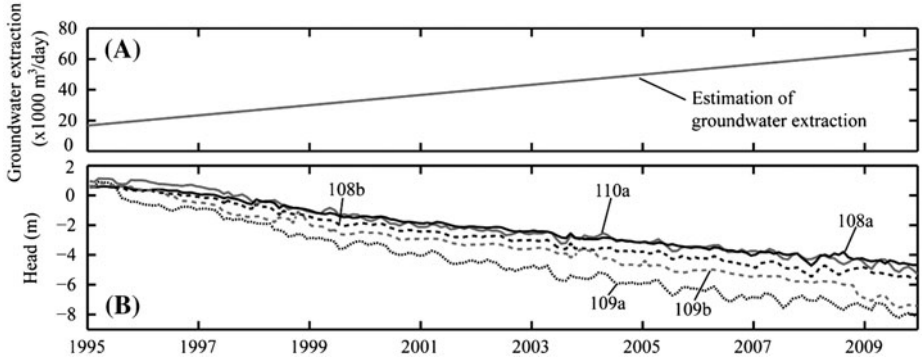

Fig. 4. (A) Estimation of groundwater extraction; and (B) records of groundwater level declinations in confined aquifers.

Table 1
Number of UNICEF wells in six districts of Nam Dinh Province

District	1998	2009
Nghia Hung	23,542	58,850
Hai Hau	26,267	65,670
Giao Thuy	2,931	7,330
Xuan Truong	4,031	10,080
Nam Truc	2,156	53,930
Truc Ninh	7,673	19,180
Total	66,660	215,040

Note: (Source: [15]).

explains the dramatic decrease in water levels in confined aquifers (Fig. 4).

Data availability on groundwater withdrawal in Nam Dinh Province is quite limited. There are no official data on the history of groundwater extraction and the location of extraction wells. For modeling purpose, the estimation of groundwater extraction is made based on the number of UNICEF wells and the population of each village. Assuming the pumping rate from each UNICEF well is 0.4 m^3/d, the total groundwater extraction for a given year is calculated. We substitute the UNICEF wells at a village with a large well located at the center of the village. As a result, 142 pumping wells representing groundwater extraction at 142 villages were modeled.

3. Method of analysis

Over the last several decades, researchers have investigated seawater intrusion problems using various approaches and models. Comprehensive reviews on seawater intrusion problems can be found in the

literature [19,20]. There are two main approaches to analyze the problem of seawater intrusion in coastal aquifers. First, analytical solutions play an important role as an instructional tool by giving fundamental insights, even if they cannot solve "real-world" problems [7,21,22]. Second, numerical methods are applied to more complex situation. The most popular codes include SEAWAT [23–25], FEFLOW [26], and SUTRA [27] among others.

This study uses SEAWAT, which is a coupled version of MODFLOW [28] and MT3DMS [29] to assess the impacts of sea-level rise and groundwater extraction on the intrusion of seawater. SEAWAT has capability to solve three-dimensional density-dependent transient regional problems for heterogeneous anisotropic aquifers. The governing equation solved by MODFLOW routines in SEAWAT for density-dependent groundwater flow is given in terms of freshwater head:

$$\begin{aligned}&\frac{\partial}{\partial\alpha}\left\{\rho_s K_{f\alpha}\left[\frac{\partial h_f}{\partial\alpha}+\frac{(\rho_s-\rho_f)}{\rho_f}\frac{\partial Z}{\partial\alpha}\right]\right\}\\&+\frac{\partial}{\partial\beta}\left\{\rho_s K_{f\beta}\left[\frac{\partial h_f}{\partial\beta}+\frac{(\rho_s-\rho_f)}{\rho_f}\frac{\partial Z}{\partial\beta}\right]\right\}\\&+\frac{\partial}{\partial\gamma}\left\{\rho_s K_{f\gamma}\left[\frac{\partial h_f}{\partial\gamma}+\frac{(\rho_s-\rho_f)}{\rho_f}\frac{\partial Z}{\partial\gamma}\right]\right\}\\&=\rho_s S_f\frac{\partial h_f}{\partial t}+\theta\frac{\partial\rho_s}{\partial C}\frac{\partial C}{\partial t}-\bar{\rho}q_s\end{aligned}\tag{1}$$

where α, β, γ, orthogonal coordinate axes, aligned with the principal directions of permeability; $K_{f\alpha}$ $K_{f\beta}$, $K_{f\gamma}$, equivalent freshwater hydraulic conductivities in the three coordinate directions, respectively [LT^{-1}]; ρ_s, fluid density [ML^{-3}]; ρ_f, density of freshwater [ML^{-3}]; h_f, equivalent freshwater head [L]; Z, elevation above datum of the center of a model cell [L]; S_f, equivalent freshwater specific storage [L^{-1}]; θ, effective porosity [dimensionless]; C, solute concentration [ML^{-3}]; $\bar{\rho}$, density of water entering from a source or leaving through a sink [ML^{-3}]; q_s, volumetric flow rate of sources or sinks per unit volume of aquifer [T^{-1}]; t, time [T].

The transport of solute mass in groundwater can be described by the following partial differential equation:

$$\frac{\partial C}{\partial t}=\nabla\cdot(D\cdot\nabla C)-\nabla\cdot(\bar{v}C)-\frac{q_s}{\theta}C_s+\sum_{k=1}^{N}R_k\tag{2}$$

where D, hydrodynamic dispersion coefficient [$L^2\ T^{-1}$]; $\bar{v}$, fluid velocity [LT^{-1}]; C_s, solute concentration of water entering from sources or sinks [ML^{-3}]; R_k (k = 1, …, N), rate of solute production or decay in reaction k of N different reactions [$ML^{-3}\ T^{-1}$].

In this study, fluid density ρ_s is assumed to be a linear function of the salt concentration: $\rho_s=\rho_f+0.7134C_s$. The effects of temperature and viscosity on fluid density are neglected. TDS is the proxy for salinity because of their correlation. Fresh water is assumed to have TDS concentration 0 g/L, while seawater is assumed to have a TDS concentration 35 g/L. Seawater intrusion is estimated by the landward migration of the 1 g/L TDS line, a concentration of dissolved salts that makes groundwater unsuitable for human use.

The estimation of the sea-level rise on the Gulf of Tonkin up to year 2100 is made by updating values of sea side boundaries every year by a simple linear equation: Stage (at sea side boundaries) = Stage (baseline 1995) + Sea-level rise (1 cm per year). We also use the river package, the recharge package, and well package of MODFLOW to simulate the hydrologic system and groundwater extraction for the study. Readers are referred to [30] for more details about these packages.

The preconditioned conjugate gradient (PCG2) solver with matrix preconditioning method of the modified incomplete Cholesky was chosen to solve transient groundwater flow equations in MODFLOW. Also, the explicit third-order total variation diminishing scheme was used to solve the advection term in order to minimize numerical dispersion which comes from implicit finite-different solution method [25].

4. Numerical setup for simulation of seawater intrusion

The study uses data from 56 boreholes in the Nam Dinh Province and its vicinity to generate the mesh. The area is discretized with 96 columns and 110 rows. Each cell is 500 m × 500 m. Six layers are used to discretize the aquifer system that extends from the land surface to a uniform depth of −210 m below the mean sea level. Model layers 1–3 correspond to the Holocene aquifers. Layer 4 is the Pleistocene aquitard. Layers 5 and 6 represent the Pleistocene confined aquifer (Fig. 5).

We used average hydrogeological conditions of 1995 for initial conditions. Initial heads were set from 0.01 to 0.96 m for all variable-head cells based on the observed heads of 1995. Initial concentrations were obtained from [16], providing information regarding the location of saline water in confined aquifers. The initial concentration of fresh water area was set as 0.5 g/L.

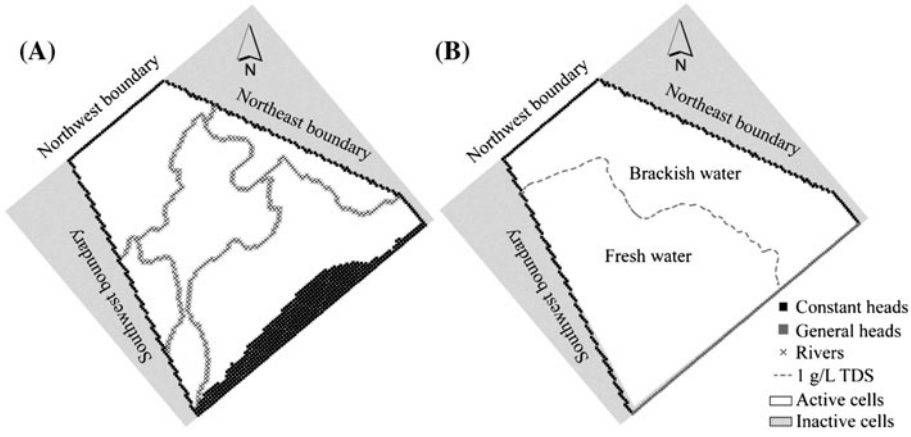

Fig. 5. Model discretization for (A) layer 1 and for (B) layers from layer 2 to layer 6. The gray-dash is the 1 g/L TDS contour line of 1999 that defines the freshwater/brackish water boundary in confined aquifers.

Since the SEAWAT model simultaneously simulates groundwater flow and solute transport, boundary conditions for these two processes are required. The boundary conditions for the flow model consist of the time-variant specified head (CHD), general-head boundary (GHB), well-field withdrawals, river, no-flow boundary, and recharge. For transport model, boundary conditions are specified for concentration and no mass-flux boundary.

To represent the stage at the Gulf of Tonkin, we assign CHD for the cells with center elevations above the Gulf of Tonkin ocean floor. The elevation of the ocean floor are determined from a bathymetric map ETOPO1 [31]. The stage is set equal to zero in 1995 with a TDS concentration of 35 g/L (Fig. 5(A)). The CHD are also assigned for the lateral boundaries on the northeast, the southwest and the northwest of the study area, which represent the groundwater interactions of the study area with its vicinity (Fig. 5(A) and (B)).

To represent the hydraulic connection of the Gulf of Tonkin stage to lower aquifers, we assign GHB for the cells at the ocean side of layer 2–6 (Fig. 5(B)). The head values for GHB cells in 1995 are set to zero and increase with the same rate as the rising sea level. TDS concentration for GHB cells are 35 g/L for all simulations. The upper boundary of the model is the water table, which is a free-surface boundary that is subject to spatially in homogeneous and time-varying recharge. Due to the scarcity of data, this study considers the recharge rate as a model parameter to be optimized through model calibration. We take four major rivers in the first layer of the model as head-dependent flux boundaries (Fig. 5(A)). The water levels and TDS for each river cell are interpolated based on the observed data.

Simulation of both freshwater and saltwater flow requires an initial estimate of the freshwater/saltwater interface altitude. The better this estimate is, the less the simulation time required to achieve the stable solution will be. This study assumes that the initial location of freshwater/saltwater interface is at the seaside boundary from layer 1 to layer 6.

4.1. Model calibration and validation

To minimize fitting errors and estimate model parameters, we use the derivative-free global optimization method CMA-ES [32,33]. The model parameters estimated are hydraulic conductivity, specific storage, specific yield, hydraulic conductance, and recharge rate (Table 2). The ranges for each parameter are based on available information such as aquifer tests, lithology and geologic data reported [14,15]. The model is calibrated over an 11-year period from 1995 to 2005, which was divided into 132 stress periods of one month each. The model is validated using an additional four-year data-set from 2006 to 2009.

A data-set of 16,597 hydraulic head records from 10 national monitoring wells (Fig. 1) were used for calibration, and another data-set of 7,617 hydraulic heads were used for validation. Fig. 6 illustrates the comparison between calculated and observed heads. The overall RMSE for calibration and validation are 0.44 m and 0.36 m, respectively. Given that the seasonal head fluctuates about 0.51 m, it is believed that a good quality model is setup which can be used for prediction purposes. Table 3 lists the optimized parameters for the flow model.

Table 2
Parameter ranges for model calibration, and parameters from previous studies

Parameters	Range		Ref. [15]	Ref. [14]
	Lower	Upper		
Horizontal hydraulic conductivity (m/d)				
Layer 1 and layer 3	1	6	1.62 and 1.45	0.5
Layer 5 and layer 6	1	15	7.75 and 1.54	40
Layer 2 and layer 4	5×10^{-4}	10^{-2}	0.003	0.0017
Specific yield (–)	10^{-2}	0.3	–	0.07
Storage coefficient (1/m)				
Layer 1, layer 3, layer 5, and layer 6	10^{-5}	10^{-3}	1.6×10^{-6} to 10^{-4}	0.001
Layer 2 and layer 4	10^{-8}	10^{-5}	3×10^{-8}	–
Vertical anisotropy (–)	10	100	1 to 100	10–100
Recharge (m/d)	10^{-5}	10^{-4}	–	–

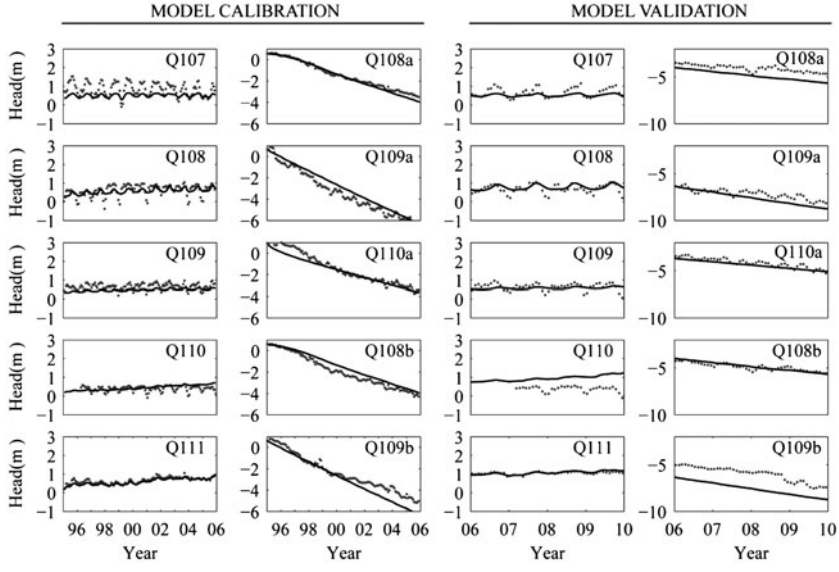

Fig. 6. Comparison between calculated (solid lines) and observed heads (scatter points).

Table 3
Optimized parameters for groundwater flow model

Parameters	Layer					
	1	2	3	4	5	6
Horizontal hydraulic conductivity (m/d)	4.80	8.79×10^{-3}	4.91	4.16×10^{-3}	14.89	8.97
Specific yield (–)	0.21	–	–	–	–	–
Storage coefficient (1/m)	2.20×10^{-6}	1.06×10^{-6}	3.90×10^{-6}	4.26×10^{-6}	1.73×10^{-5}	2.05×10^{-4}
Vertical anisotropy (–)	17.25	56.20	13.16	62.06	19.58	15.94
Recharge rate (m/d)	*1.69×10^{-5}	–	–	–	–	–
	**1.20×10^{-5}	–	–	–	–	–

*Dry season (Layers 1, 2, 3); **Wet season (Layers 4, 5, 6).

Table 4
Summary of simulation scenarios for prediction of seawater intrusion

Scenario	Groundwater extraction	Sea level
Scenario 1	Same as in January 2010 (Q_1 = 66,506 m^3/d)	Rise up to 1 m by 2100 with respect to 1980–1999
Scenario 2	Linear increase during 2010–2050 with the same rate as 1995–2010. After 2050, pumping rate is kept constant (Q_2 = 199,395 m^3/d)	Rise up to 1 m by 2100 with respect to 1980–1999
Scenario 3	Same as scenario 2	No sea-level rise

4.2. Scenarios for simulation of seawater intrusion

By tracking the movement of 1 g/L TDS line, we can measure the impacts of groundwater extraction and sea-level rise on the extent of seawater. The baseline scenario corresponds to the 2010 conditions. The groundwater pumping is 66,507 m^3/d. The sea level is at 7 cm above the mean sea level. We consider three different scenarios of sea-level rise and groundwater extraction (Table 4). To predict the extent of seawater, we ran the SEAWAT model over the 90 years into the future under the following assumptions: (a) hydraulic parameters remain the same as in Table 3; (b) future hydrologic conditions are the same as in calibration period; and (c) the tidal effect and the change of shoreline are neglected.

Due to the scarcity of measured TDS concentrations, no effort was made to calibrate the transport model. Instead, we investigate the extent and the intrusion mechanism of seawater through sensitivity analysis for transport parameters including dispersivity and porosity. Initially, the longitudinal dispersivity is assigned a value of 50 m [6,34]. The ratio of the horizontal transverse dispersivity to the longitudinal dispersivity is 0.1, while the ratio of the vertical transverse dispersivity to the longitudinal dispersivity is 0.01. The diffusion coefficient and effective porosity are 2×10^{-5} m^2/d and 0.3, respectively.

5. Results and discussion

5.1. Groundwater flow

Using simulation results of hydrological year 2009, we analyze the waterbudget, the river-aquifer interaction, and the recharge into the aquifer system. We focus on the upper unconfined aquifer (layer 1) and the fresh water area in the confined aquifer (layer 5).

For the upper unconfined aquifer, inflow components include recharge, flow from river, and flow from four boundaries (northwest, northeast, southeast, and the ocean). Outflow components include flow to river, flow to lower aquiclude (layer 2), and flow to four boundaries. The average water budget for the upper unconfined aquifer (layer 1) in a dry season (October 2008 to May 2009) and a wet season (June to September 2009) are presented in Fig. 7(A and B) and (C and D), respectively.

Results show an active interaction between the rivers and the upper unconfined aquifer. In a wet season, when the water levels in the river are high, the river systems supply water to the aquifer. In contrast, in a dry season, the upper unconfined aquifer provides water to the river system. Meanwhile, results also show a limited interaction of upper unconfined aquifer with the surrounding medium in both seasons.

For fresh water areas in the confined aquifer (layer 5), inflow components include brackish water from the north, seawater from the ocean, fresh water from the southwest, freshwater from the upper aquitard (layer 4), and freshwater from the lower aquifer (layer 6). Outflow components include well extractions, flow to the southwest, flow to the ocean, and flow to the lower aquifer. Fig. 7(E) and (F) represents the average flow in and out of the fresh water area in the confined aquifer.

The largest input to the fresh water area is from the lower aquifer (layer 6) (Fig. 7(E)). Also, seawater intruded from the sea and brackish water migrated from the north accounts for the significant portion. In 2009, the fresh water area receives 16,838 m^3/d (21% of total inflow) of seawater, and 10,027 (m^3/d) (13% of total inflow) of brackish water.

Regarding the outflow of the fresh water area, pumping extracts most of the water. Nearly half of the remaining water flows to the southeast, and the rest goes to the lower aquifer (Fig. 7(F)).

5.2. Effects on groundwater level

Fig. 8(A) shows the hydraulic heads in the confined aquifer (layer 5) for the predevelopment condition (1995) and after 15 years of groundwater

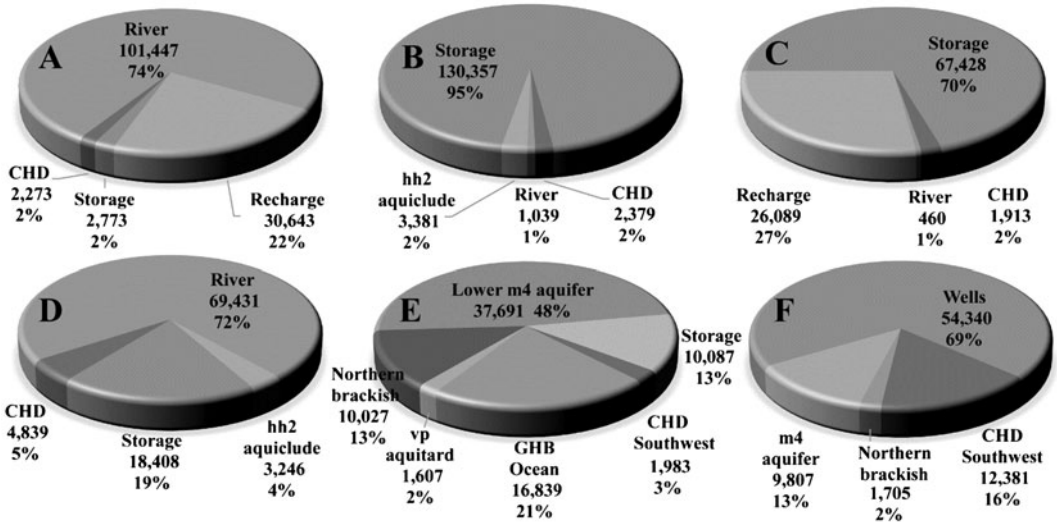

Fig. 7. Flow budget for hydrological year 2009: (A) and (B) are flow in/out for upper unconfined aquifer (layer 1) in wet season; (C) and (D) are flow in/out for upper unconfined aquifer (layer 1) in dry season; (E) and (F) are flow in/out for fresh water area in confined aquifer (layer 5). The numbers are average flow rate (m^3/d) and percentage.

pumping (2010), including the impacts of sea-level rise. The pumping rate in 2010 is 66,506 m^3/d, which is approximately four times larger than 16,673 m^3/d of 1995. Due to the increase in groundwater pumping, a cone of depression has developed in the area with the largest pumping rate. At observation well Q109, the hydraulic head has decreased from 0.75 m in 1995 to −8 m in 2010, showing a relatively fast lowering speed of 0.55 m/y.

Fig. 8(B) and (C) illustrates the predicted impacts of low pumping rate (scenario 1) and high pumping rate (scenario 2) on the groundwater levels in 2050. As for scenario 1, Q_1 = 66,506 m^3/d as in 2010, a cone of depression over −12 m is formed at the major

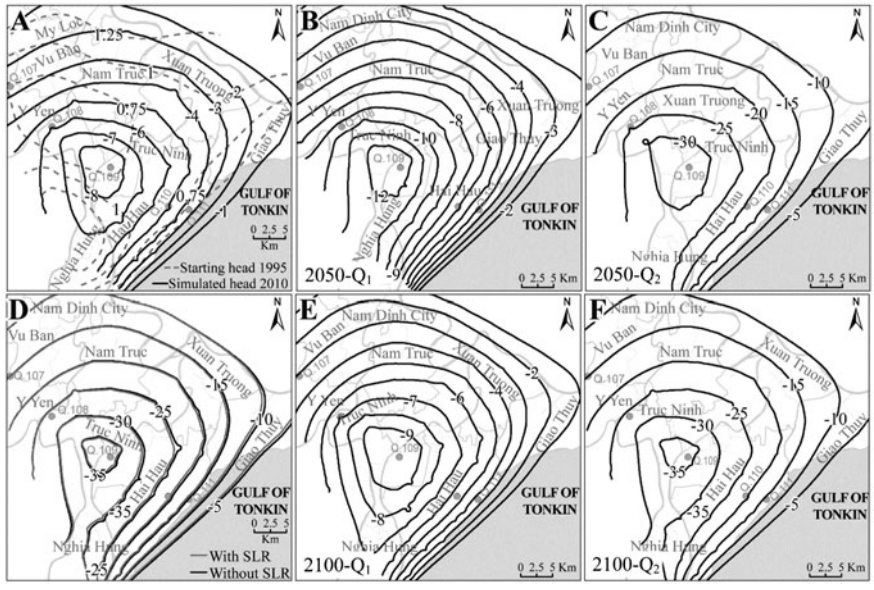

Fig. 8. Distribution of groundwater levels in confined aquifer (layer 5): (A) predevelopment condition in 1995 and simulated groundwater levels in 2010; (B) and (C) the predicted groundwater levels in 2050 for low pumping rate Q_1 and high pumping rate Q_2; (E) and (F) are the predicted groundwater levels in 2100 for low pumping rate Q_1 and high pumping rate Q_2; and (D) Influence of SLR on groundwater level in 2100.

pumping wells (Fig. 8(B)). The predicted groundwater level at observation well Q109 in 2050 is 4 m lower than that of 2010, showing a slow decreasing speed (0.08 m/y). In scenario 2, with the linear increase in pumping up to Q_2 = 199,395 m^3/d, the cone of depression is more than −30 m below the mean sea level (Fig. 8C). The intensive groundwater pumping creates a hydraulic gradient of 1.44 m/km from observation well Q111 to Q109, which is much larger than that of 0.07 m/km in 1995.

Predictions are made further into the year 2100. In case of low pumping rate (Q_1 = 66,506 m^3/d), we find a recovery of groundwater level (Fig. 8(E)). By 2100, the cone of depression rises about 3 m, showing a similar head distribution as in 2010. However, if we maintain the high pumping rate Q_2 = 199,395 m^3/d during 2050–2100 (scenario 2), the ground water level will keep decreasing. The predicted groundwater level is lower than −35 m below the mean sea level in the area of largest pumping (Fig. 8(F)).

Fig. 8(D) reveals the influence of sea-level rise to the groundwater level. The contribution of a sea-level rise from 0 m to 1 m in 2100 to the groundwater level is expected to be relatively small. Simulation results indicate that the groundwater level increases 0.29 m at observation well Q109, which is 14.4 km away from the seashore. At observation well Q110, 3.4 km away from the seashore, the groundwater level increase will be 0.65 m. Our results are consistent with the previous finding [35] that the sea-level rise will slightly raise the entire freshwater body by a mechanism identified as the "lifting process".

5.3. Effects on freshwater/saltwater interface

As stated earlier, we measure the movement of freshwater/seawater interface by tracking the movement of 1 g/L TDS line. Fig. 9(A) presents the predicted extent of 1 g/L TDS lines for two pumping scenarios in 2100. For low pumping rate case (scenario 1), a 2–3 km landward movement of the 1 g/L TDS line is obtained. For high pumping rate case (scenario 2), the landward movement of the 1 g/L TDS line becomes greater, 4–5 km. It implies that the groundwater in the districts of Nghia Hung and Hai Hau could become unusable.

We evaluated the impact of sea-level rise by comparing the 1 g/L TDS lines for scenarios 2 and 3. Results indicated a minor impact of sea-level rise on the fresh water area in the confined aquifer (layer 5). Fig. 9(F) shows that the 1 g/L TDS line for scenario 2 (with 1 m sea-level rise) moved several hundred meters inland, in contrast with no sea-level rise scenario. This result is also consistent with findings from the previous studies [6,7,24].

To better understand the seawater intrusion mechanism, we conducted sensitivity analysis. The

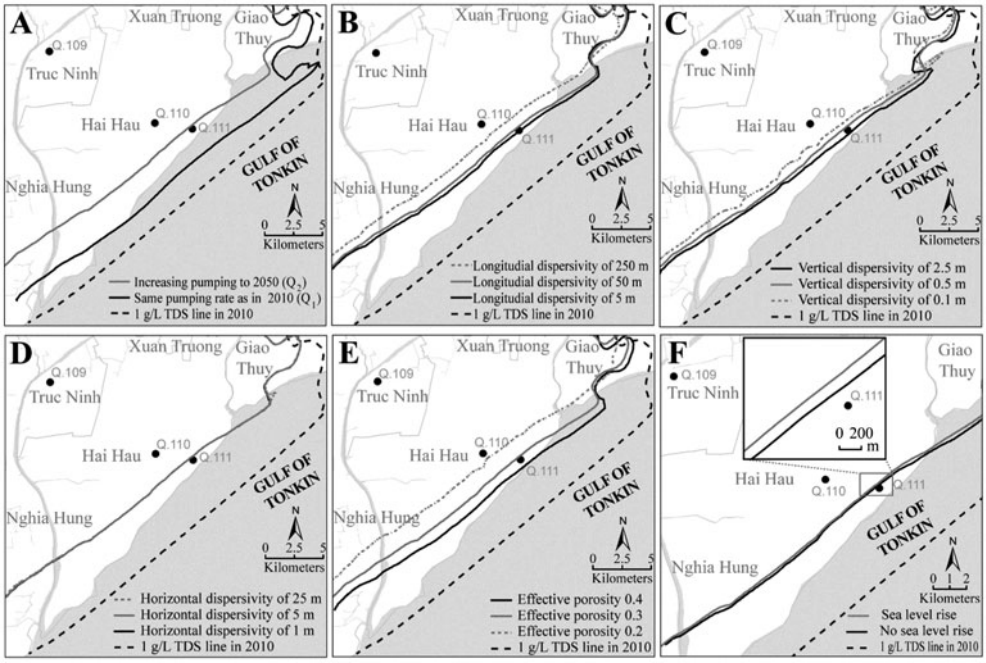

Fig. 9. Sensitivity of 1 g/L TDS line in 2100 to: (A) pumping rate; (B) longitudinal dispersivity; (C) vertical transverse dispersivity; (D) horizontal transverse dispersivity; (E) effective porosity; and (F) sea-level rise.

Table 5
Range of transport parameters for sensitivity analysis

Parameter	Baseline	Low	High
Longitudinal dispersivity (m)	50	5	250
Horizontal transverse dispersivity (m)	5	1	25
Vertical transverse dispersivity (m)	0.5	0.1	2.5
Diffusion coefficient (m^2/d)	2×10^{-5}	2×10^{-5}	2×10^{-5}
Effective porosity	0.3	0.2	0.4

movement of 1 g/L TDS lines for different scenarios was tracked. Scenario 2 served as a baseline case, and the transport parameters were varied (Table 5).

Results show that longitudinal dispersivity, vertical transverse dispersivity, and effective porosity have large effects on the landward movement of 1 g/L TDS line. By increasing the longitudinal dispersivity from 50 to 250 m, the 1 g/L TDS line migrated approximately 1.5 km landward. By reducing the longitudinal dispersivity from 50 to 5 m, the 1 g/L TDS line retreated several hundred meters toward the sea (Fig. 9(B)). An increase in the vertical transverse dispersivity from 0.5 to 2.5 m showed about 1.1 km landward movement of the 1 g/L TDS line, while a decrease to 0.1 m yielded a seaward retreat of several hundred meters (Fig. 9(C)). As for the effective porosity, a 33% decrease from the baseline value resulted in 2.4 km inland intrusion of the 1 g/L TDS line, while a 33% increase resulted in 1 km seaward retreat (Fig. 9(E)). Horizontal transverse dispersivity was insensitive and had minor impacts on the intrusion of seawater (Fig. 9(D)). The analysis suggests that the proper estimation of transport parameters is critical for the reliable assessment of seawater intrusion.

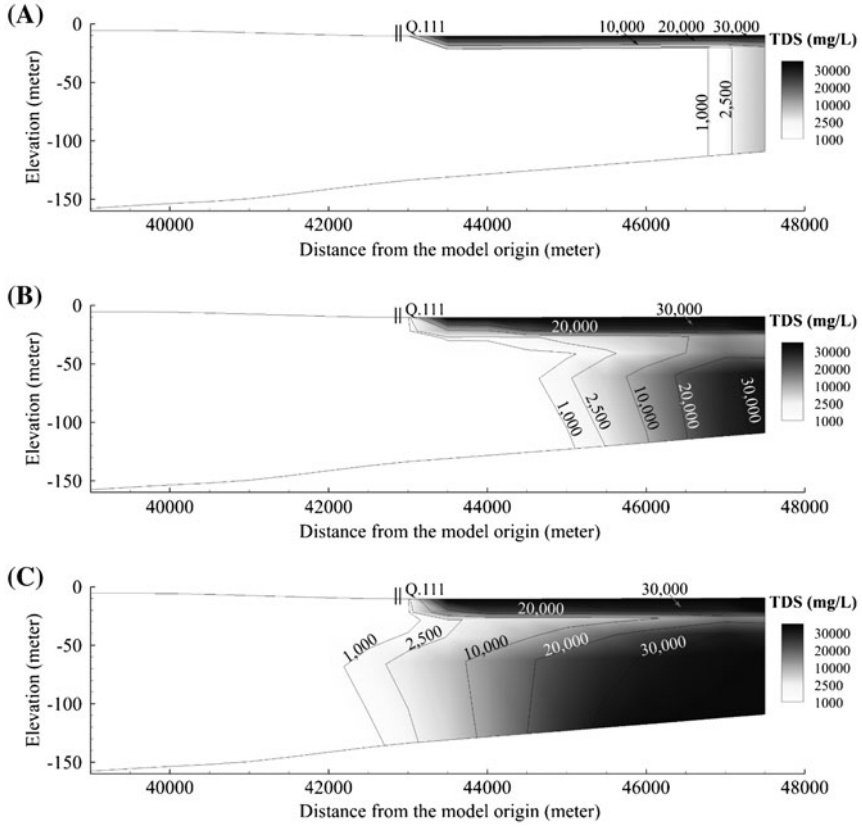

Fig. 10. The TDS lines at cross-section passing observation well Q111 for: (A) Year 2010; (B) Year 2100 with low pumping rate Q_1; and (C) Year 2100 with high pumping rate Q_2. Vertical exaggeration is 15 times.

Due to the flat nature of the river delta in the coastal area of the Nam Dinh Province, the rise of the sea level would cause significant landward movement of seawater. With a 1 m rise of the sea level by 2100, about 93.4 km^2 of coastal area accounting for 5.7% of the province, would be permanently inundated [36]. Consequently, the upper unconfined aquifer of Nam Dinh coastal area, which is already in high salt concentration, would become saltier. The high TDS concentration in the upper unconfined aquifer, however, would not significantly affect the fresh water in the confined aquifers (layer 5 and layer 6). By comparing the 1 g/L TDS lines for scenarios 1 and 2 (Fig. 10(B) and (C)) against the baseline (Fig. 10(A)), we find several meters of downward movement in the 1 g/L TDS lines, which is relatively small in comparison with several kilometers of landward movement in the horizontal direction. It is because the confined aquifers (layer 5 and layer 6) and the upper aquifers (layer 1 and layer 3) are separated by low permeability aquitards (layer 4 and layer 2). Therefore, the potential migration of salt water from the upper unconfined aquifer to the fresh water area in the confined aquifer (layer 5) would be insignificant.

6. Conclusions

This study investigated the potential impact of rising sea levels and groundwater extraction on the seawater intrusion in the Nam Dinh coastal aquifers of Vietnam. To understand the seawater intrusion mechanism in the region, an effort was made to model the complete hydrogeological system numerically.

The derivative-free global optimization scheme CMA-ES turned out to be useful for model calibration, yielding a good match between observed and simulated groundwater levels. The extent of seawater intrusion to the year 2100 was predicted under various groundwater extraction and sea-level rise scenarios.

Interaction between the river system and groundwater in the upper aquifers was found to be active. But, vertical water exchange between aquifers was limited. The extraction of groundwater was the key factor causing the groundwater drawdown and seawater intrusion in Nam Dinh coastal aquifers. Rising sea levels will lift up the entire freshwater body, but its effect on the seawater intrusion will be minor. Parameter analysis indicates that the movement of seawater is sensitive to longitudinal transverse dispersivity, vertical transverse dispersivity, and effective porosity. Further studies are needed to reduce the uncertainties in transport parameters.

Acknowledgment

This work was done while the first author was a graduate student at Dongguk University. Authors are grateful for the support from the National Research Foundation of Korea (NRF) under the contract number 2013052502.

Symbols and abbreviations

α, β, γ	—	orthogonal coordinate axes aligned with the principal directions of permeability
ρ_f	—	freshwater density, ML^{-3}
ρ_s	—	fluid density, ML^{-3}
θ	—	effective porosity [dimensionless]
$\bar{\rho}$	—	density of water entering from a source or leaving through a sink, ML^{-3}
h_f	—	equivalent freshwater head, L
q_s	—	volumetric flow rate of sources or sinks per unit volume of aquifer, T^{-1}
t	—	time, T
$\bar{v}$	—	fluid velocity, LT^{-1}
C	—	solute concentration, ML^{-3}
C_s	—	solute concentration of water entering from sources or leaving through sinks, ML^{-3}
D	—	hydrodynamic dispersion coefficient, $L^2\,T^{-1}$
$K_{f\alpha}, K_{f\beta}, K_{f\gamma}$	—	equivalent freshwater hydraulic conductivities in the three coordinate directions, respectively, LT^{-1}
R_k	—	rate of solute production or decay in reaction k of N different reactions, $ML^{-3}\,T^{-1}$.
S_f	—	equivalent freshwater specific storage, L^{-1}
Z	—	elevation above datum of the center of a model cell, L
CHD	—	time-variant specified head
CMA-ES	—	covariance matrix adaptation–evolution strategy
CWRPI	—	the National Centre for Water Resources Planning and Investigation
GHD	—	general-head boundary
MONRE	—	Ministry of Natural Resources and Environment
RMSE	—	root mean squared error
TDS	—	total dissolved solids
UNICEF	—	the United Nations Children's Fund
USGS	—	US Geological Survey

References

[1] C.J.G. Darnault (Ed.), Overexploitation and Contamination of Shared Groundwater Resources, Springer, Netherlands, Dordrecht, 2008.
[2] M.M. Sherif, V.P. Singh, Effect of climate change on sea water intrusion in coastal aquifers, Hydrol. Processes 13 (1999) 1277–1287.

[3] A.G. Bobba, Numerical modelling of salt-water intrusion due to human activities and sea-level change in the Godavari Delta, India, Hydrol. Sci. J. 47 (2002) S67–S80.
[4] J.F. Carneiro, M. Boughriba, A. Correia, Y. Zarhloule, A. Rimi, B.E. Houadi, Evaluation of climate change effects in a coastal aquifer in Morocco using a density-dependent numerical model, Environ. Earth Sci. 61 (2010) 241–252.
[5] Y. Yechieli, E. Shalev, S. Wollman, Y. Kiro, U. Kafri, Response of the Mediterranean and Dead Sea coastal aquifers to sea level variations, Water Resour. Res. 46 (2010) W12550.
[6] H.A. Loáiciga, T.J. Pingel, E.S. Garcia, Sea water intrusion by sea-level rise: Scenarios for the 21st century, Ground Water 50(1) (2012) 37–47.
[7] A.D. Werner, C.T. Simmons, Impact of sea-level rise on sea water intrusion in coastal aquifers, Ground Water 47(2) (2009) 197–204.
[8] W.E. Sanford, J.P. Pope, Desafios actuais no uso de modelos de previsão da intrusão marinha: lições da Costa Leste (Eastern Shore) da Virgínia, EUA (Current challenges using models to forecast seawater intrusion: lessons from the Eastern Shore of Virginia, USA), Hydrogeol. J. 18 (2010) 73–93.
[9] R.J. Nicholls, N. Mimura, Regional issues raised by sea-level rise and their policy implications, Clim. Res. 11 (1998) 5–18.
[10] S. Dasgupta, B. Laplante, C. Meisner, D. Wheeler, J. Yan, The impact of sea level rise on developing countries: A comparative analysis, Clim. Change 93 (2008) 379–388.
[11] MONRE, Climate Change Scenarios, Sea Level Rise for Vietnam, Vietnam Publishing House of Natural Recourses, Environment and Cartography, Hanoi, 2012.
[12] D.T. Tran, Y. Saito, V.H. Dinh, V.L. Nguyen, T.K.O. Ta, M. Tateishi, Regimes of human and climate impacts on coastal changes in Vietnam, Reg. Environ. Change 4 (2004) 49–62.
[13] C. Jolk, S. Greassidis, S. Jaschinski, H. Stolpe, B. Zindler, Planning and decision support tools for the integrated water resources management in Vietnam, Water 2 (2010) 711–725.
[14] V.C. Doan, T.L. Le, V.H. Hoang, D.R. Nguyen, V.N. Nguyen, Groundwater resource of Nam Dinh province, J. Geol. Ser. B 25 (2005) 31–43.
[15] F. Lindenmaier, R. Bahls, F. Wagner, Assessment of Groundwater Resources in Nam Dinh Province-Final Technical Report, Part B, Federal Ministry for Economic Cooperation and Development, Hanoi, 2011.
[16] F. Wagner, T.T. Dang, D.P. Hoang, F. Lindenmaier, Assessment of Groundwater Resources in Nam Dinh Province-Final Technical Report, Part A, Federal Ministry for Economic Cooperation and Development, Hanoi, 2011.
[17] H. Bui, T.L. Le, M.T. Schafmeister, K.H. Pham, B.V. Do, Application of isotopic hydrogeological methods to investigate groundwater in Nam Dinh area, J. Geol. 21(B) (2003) 88–94.
[18] L.T. Tran, F. Larsen, N.Q. Pham, A.V. Christiansen, N. Tran, H.V. Vu, L.V. Tran, H.V. Hoang, K. Hinsby, Origem e extensão das águas doces subterrâneas, das paleoáguas salgadas e das intrusões marinhas recentes nos aquíferos da planície inundável do Rio Vermelho, Vietname (Origin and extent of fresh groundwater, salty paleowaters and recent saltwater intrusions in Red River flood plain aquifers, Vietnam), Hydrogeol. J. 20(7) (2012) 1295–1313.
[19] J. Bear, A.H.-D. Cheng, S. Sorek, D. Ouazar, I. Herrera, Seawater Intrusion in Coastal Aquifers: Concepts, Methods, and Practices, Kluwer Academic Publishers, Dordrecht, The Netherlands, 1999.
[20] A.D. Werner, M. Bakker, V.E.A. Post, A. Vandenbohede, C. Lu, B. Ataie-Ashtiani, Seawater intrusion processes, investigation and management: Recent advances and future challenges, Adv. Water Res. 51 (2013) 3–26.
[21] S. Carretero, J. Rapaglia, H. Bokuniewicz, E. Kruse, Impact of sea-level rise on saltwater intrusion length into the coastal aquifer, Partido de La Costa, Argentina, Cont. Shelf Res. 61–62 (2013) 62–70.
[22] K. Mazi, A.D. Koussis, G. Destouni, Tipping points for seawater intrusion in coastal aquifers under rising sea level, Environ. Res. Lett. 8 (2013) 014001.
[23] J.P. Masterson, S.P. Garabedian, Effects of sea-level rise on ground water flow in a coastal aquifer system, Ground Water 45(2) (2007) 209–217.
[24] P. Rasmussen, T.O. Sonnenborg, G. Goncear, K. Hinsby, Assessing impacts of climate change, sea level rise, and drainage canals on saltwater intrusion to coastal aquifer, Hydrol. Earth Syst. Sci. 17 (2013) 421–443.
[25] C.D. Langevin, D.T. Thorne Jr, A.M. Dausman, M.C. Sukop, W. Guo, SEAWAT Version 4: A Computer Program for Simulation of Multi-Species Solute and Heat Transport, US Geological Survey, Reston, VA, 2008.
[26] T.A. Watson, A.D. Werner, C.T. Simmons, Transience of seawater intrusion in response to sea level rise, Water Resour. Res. 46 (2010) W12533.
[27] J.D. Hughes, H.L. Vacher, W.E. Sanford, Temporal response of hydraulic head, temperature, and chloride concentrations to sea-level changes, Floridan aquifer system, USA, Hydrol. J. 17 (2008) 793–815.
[28] A.W. Harbaugh, R.B. Edward, M.C. Hill, M.G. McDonald, MODFLOW-2000, the US Geological Survey Modular Ground-water Model: User Guide to Modularization Concepts and the Ground-water Flow Process, US Geological Survey, Reston, VA, 2000.
[29] C. Zheng, P.P. Wang, MT3DMS, A Modular Three-Dimensional Multi-species Transport Model for Simulation of Advection, Dispersion, and Chemical Reactions of Contaminants in Ground-water Systems: Documentation and User's Guide, US Army Engineer Research and Development Center Contract Report SERDP-99-1, Vicksburg, MS, 1999.
[30] A.W. Harbaugh, MODFLOW-2005, The US Geological Survey Modular Ground-Water Model—the Ground-water Flow Process, in: Book 6. Modeling Techniques, Section A. Ground Water, US Geological Survey, Reston, VA, 2005.
[31] C. Amante, B. Eakins, ETOPO 1 1Arc-minute Global Relief Model: Procedures, Data Sources and Analysis, National Geophysical Data Center, NOAA, Boulder, CO, 2009.
[32] N. Hansen, A. Ostermeier, Completely derandomized self-adaptation in evolution strategies, Evol. Comput. 9 (2001) 159–195.

[33] N. Hansen, S.D. Müller, P. Koumoutsakos, Reducing the time complexity of the derandomized evolution strategy with covariance matrix adaptation (CMA-ES), Evol. Comput. 11 (2003) 1–18.
[34] M. Cobaner, R. Yurtal, A. Dogan, L.H. Motz, Three dimensional simulation of seawater intrusion in coastal aquifers: A case study in the Goksu Deltaic Plain, J. Hydrol. 464–465 (2012) 262–280.
[35] S.W. Chang, T.P. Clement, M.J. Simpson, K.-K. Lee, Does sea-level rise have an impact on saltwater intrusion? Adv. Water Resour. 34 (2011) 1283–1291.
[36] J. Carew-Reid, Rapid Assessment of the Extent and Impact of Sea Level Rise in Vietnam, Climate Change Discussion Paper 1, ICEM—International Centre for Environment Management, Brisbane, 2007.